Robust Real-Time Distributed Optimal Control Based Energy Management in a Smart Grid

Yinliang Xu, *Member, IEEE*, Zaiyue Yang, *Member, IEEE*, Wei Gu, *Member, IEEE*, Ming Li, *Member, IEEE*, and Zicong Deng

***Abstract*—With the integration of distributed generations and controllable loads, the power grid becomes geographically distributed with a time-varying topology. The operation conditions may change rapidly and frequently; thus, management and control of the smart grid pose great challenges on traditional centralized control strategies. This paper proposes a distributed algorithm for energy management in a power grid, while dynamically minimizing the adjustment costs. The objective function is designed to optimize the overall social welfare considering generation suppliers and load users simultaneously. The proposed algorithm integrates consensus algorithm and optimal control algorithm, which requires only information exchanging among neighboring units and enables the sharing of computational and communication burden among distributed local controllers. It is robust to communication failures and adaptive to topology changes. Simulation results of the IEEE 9-bus, 39-bus systems, and a 200-unit system demonstrate the effectiveness of the proposed algorithm and indicate the promising applications to practical power systems.**

***Index Terms*—Distributed algorithm, optimal control, energy management, consensus algorithm, smart grid.**

Nomenclature

P_{Gi}	Distributed generation at bus i
P_{Li}	Load demand at bus i
$\alpha_i, \beta_i, \gamma_i$	Fuel cost coefficients of generator i
σ_i, ω_i	Benefit coefficients of load user i
w_i	Incremental cost of unit i
w^*	Optimal incremental cost
x_i	State variable
u_i	Control variable
J_i	Local objective function
l_{ij}	Communication coefficient between i and j
$\lambda(t)$	Lagrange multiplier at time t
e, m, f, r	Weight coefficients for dynamic coordination
ϵ	Step size
Δt	One control cycle for real-time implementation
P'_{Di}	Local estimated supply-demand mismatch
P_{Di}	Global supply-demand mismatch
$\mathbf{Q}$	Weight matrix for state variable
$\mathbf{R}$	Weight matrix for control variable
$\mathbf{S}(T)$	Weight matrix for the final state

Manuscript received May 2, 2015; revised July 24, 2015 and September 8, 2015; accepted October 11, 2015. Date of publication November 3, 2015; date of current version June 19, 2017. This work was supported by the National Natural Science Foundation of China under Grant 51507193. Paper no. TSG-00496-2015. *(Corresponding author: Yinliang Xu.)*

Y. Xu, M. Li, and Z. Deng are with the Sun Yat-sen University–Carnegie Mellon University (SYSU–CMU) Joint Institute of Engineering, Sun Yat-sen University, Guangzhou 510275, China, and also with SYSU–CMU Shunde International Joint Research Institute, Shunde 528300, China (e-mail: xuyliang@mail.sysu.edu.cn; liming46@mail.sysu.edu.cn; dengzicong@126.com).

Z. Yang is with the State Key Laboratory of Industrial Control Technology, Department of Control Science and Engineering, Zhejiang University, Hangzhou 310027, China (e-mail: yangzy@zju.edu.cn).

W. Gu is with the School of Electrical Engineering, Southeast University, Nanjing 210096, China (e-mail: wgu@seu.edu.cn).

Color versions of one or more of the figures in this paper are available online at http://ieeexplore.ieee.org.

Digital Object Identifier 10.1109/TSG.2015.2491923

I. Introduction

DRIVEN by the ever increasing energy demand, economical consideration and environmental concerns of promoting lower-carbon and high efficiency generation technology, the power industry is facing with the challenges and opportunities of transforming the present power grid into a smart grid [1], [2]. The benefits of smart grid development and deployment include helping the system manage generation-demand balance, optimizing asset utilization, improving grid reliability, reducing its environmental impact, etc. [3].

With the integration of distributed generation, energy storage system, and controllable loads, the smart grid becomes geographically distributed [4]. Due to the distributed participants' requirement of plug-and-play at arbitrary time, the smart grid topology is time-varying. Furthermore, the operation conditions may change rapidly and frequently due to the unexpected generation-demand imbalance caused by the behaviors of distributed participants [5]. Thus, management and control of the smart grid pose great challenges on traditional centralized control strategies [6], which require the collection of global information and a powerful central controller to process large amounts of data [7]. There is an increasingly demand of developing fast, flexible, scalable, reliable and cost-effective distributed solutions to address the features of smart grid [8]–[10].

With the integration of smart sensors and meters, and advanced two-way communication technology, distributed control strategy, which can effectively exploit the intelligence of local controllers and sparse communication network, seems to be a more viable option [11], [12]. Distributed management and control strategy may be a crucial enabler in smart grid technology to better accommodate distributed technologies and activate user participations [13].

Optimal management and control of power balance involve the collaboration of various participants in charge of distributed generation and load demand. An increasing level of coupling is observed, i.e., each participant, when enjoying the utilization benefit by acquiring a certain amount of power, will incur a coupled cost from the generation suppliers which will be shared by all the other users in one way or another [14]. Thus, the objective is to maximize the social welfare of all participants, including users and electrical power providers.

There exists plenty of literature on distributed strategies of optimal energy management in terms of demand response, and economic dispatch. In [15], the authors presented a distributed coordinated demand response scheme based on the prices announced by the central utility. Although the bidding process is designed in a distributed way, the central utility still needs to collect the demand requirements from all dispersed users and release the price through a central-to-local communication network. In [16], the authors proposed a distributed demand response control strategy based on Lyapunov optimization to reduce the variation of nonrenewable power demand. The proposed strategy can avoid the communication error in delivering the control decisions from the control center to local users. However, the proposed algorithm is not fully distributed because a control center is still needed to calculate aggregated power consumption.

In recent literature, numerous fully distributed control strategies, which only require information exchange among neighboring controllers, have been proposed. In [17], the authors propose a consensus based distributed strategy to economically allocate the total load demand among multiple distributed generators while respecting local inequality and global equality constraints. In [6], the authors propose a new distributed control algorithm by randomizing user demand responses to maintain the frequency of the power grid. However, these approaches are effective under the circumstance that either the total generations or the load demands are constant, which limits their application to the power balance management in smart grid. To address this issue, several fully distributed energy management approaches have been proposed. In [18], the authors devise a distributed real-time demand response in the multi-seller-multi-buyer environment by firstly decoupling into single-seller–multi-buyer subsystems. In [19], the authors present an incremental welfare consensus algorithm to coordinate distributed generation and load. The proposed distributed algorithm was validated through numerical case studies. The real time implementation still needs to be investigated. In [20], the authors propose a consensus based distributed optimal resource management to maintain the generation-demand balance in an islanded microgrid. However, the dynamic adjustment coordination of the units in the system was not considered, which is important for real time implementation since the system frequency dynamic performance will be affected.

The aforementioned distributed energy management approaches effectively minimize generation cost, maximize user benefits, and/or optimize the overall social welfare. However, to the authors' best knowledge, few studies have been carried out to minimize the generation or load demand adjustment during the dynamic process of generation-demand balancing. The dynamic adjustments can be considered as undesired disturbances to the participants. Large and abrupt adjustments will introduce various costs on different controllable devises due to their influences on wearing and life cycle [21], [22]. For the distributed algorithms to be more economical viable in smart grid real-time management and control, cost of dynamic adjustment needs to be taken into consideration.

In this paper, a distributed optimal control algorithm has been proposed to maintain the generation-demand balance in the smart grid, while dynamically minimizing the adjustment cost considering distributed dispatchable generations and responsive loads simultaneously. Each bus in the power grid is associated with a local controller, which is responsible for collecting local generation or load demand information, communicating with neighboring controllers, and updating the local control signal for local participant. The proposed distributed algorithm has been tested with the IEEE 9-bus, 39-bus and 200-unit systems, which demonstrates its effectiveness. The major features of the proposed distributed optimal control algorithm for energy management are summarized as follows:

1) The social welfare of all participants including generation suppliers and load users is optimized, while maintaining the generation-demand balance.

2) Only information exchange among neighboring controllers is required to achieve the optimal solution, and the control signal is updated by local controller. Thus, the cost of the supporting communication network can be reduced significantly and the expenditure of powerful central controller can be spared, comparing to traditional centralized control algorithms.

3) Distributed optimal control algorithm has been employed to minimize the adjustment cost during the dynamic process of balancing generation-demand.

4) The proposed algorithm is robust to communication failures and adaptive to topology changes.

5) The proposed distributed algorithm is scalable and has been verified through the simulations on the 200-unit system, which indicates its promising applications in large complex systems.

The rest of the paper is organized as follows. Section II describes the problem formulation of generation-demand balance. Section III presents the proposed distributed optimal control algorithm. Section IV discusses the simulation results of the proposed algorithm, and Section V concludes the paper.

II. Problem Formulation

The system consists of n local controllers in corresponding to n buses. Local controller is responsible for adjusting the local generation or load demand to maintain the generation-demand balance. The decision to be made at time t is how much to increase/decrease the generation or load

$$P_{Gi}(t+\Delta t) = P_{Gi}(t) + \dot{P}_{Gi}(t)\Delta t, \tag{1}$$

$$P_{Li}(t+\Delta t) = P_{Li}(t) + \dot{P}_{Li}(t)\Delta t \tag{2}$$

where $P_{Gi}(t)$ and $P_{Li}(t)$ are the distributed generation and load demand at bus i, $\dot{P}_{Gi}(t)$ and $\dot{P}_{Li}(t)$ are the associated generation and load adjustment rates, respectively.

Due to the coupled generation cost of suppliers and utility benefit of users, a suitable energy management is required to coordinate all the participants to maintain the active power balance within the power grid. On top of maintaining the generation-demand balance, the cost of the generation suppliers and load users should be well considered.

The cost function for conventional fuel generators is usually modeled as [17], [19]

$$C_i(P_{Gi}(t)) = \alpha_i P_{Gi}^2(t) + \beta_i P_{Gi}(t) + \gamma_i, \left(P_{Gi}^{\min} \leq P_{Gi}(t) \leq P_{Gi}^{\max}\right) \quad (3)$$

where the predetermined constants $\alpha_i, \beta_i, \gamma_i$, are the fuel cost coefficients, and $P_{Gi}^{\min}$, $P_{Gi}^{\max}$ are the generation lower and upper limits, respectively.

The utility benefit function of load user i is defined for aggregated load of different tasks, rather than power consumption of individual appliances. For the users, more tasks can be accomplished if more power is consumed [24], thus it is reasonable to assume the utility benefit is non-decreasing and will eventually get saturated [20], [25]

$$D_i(P_{Li}(t)) = \begin{cases} \omega_i P_{Li}(t) - \sigma_i P_{Li}^2(t) & P_{Li}^{\min} \leq P_{Li}(t) \leq \omega_i \big/ 2\sigma_i \\ \omega_i^2 \big/ 4\sigma_i & P_{Li}^{\max} \geq P_{Li}(t) > \omega_i \big/ 2\sigma_i \end{cases} \quad (4)$$

where σ_i and ω_i are the benefit coefficients of load user i, $P_{Li}^{\min}, P_{Li}^{\max}$ are the demand lower and upper bound, respectively.

The objective to maximize the social welfare is formulated as

$$\begin{aligned} \text{Maximize} \quad & -\sum_{i=1}^{n} C_i(P_{Gi}) + \sum_{i=1}^{n} D_i(P_{Li}) \\ \text{s. t.} \quad & \sum_{i=1}^{n} P_{Gi} - \sum_{i=1}^{n} P_{Li} = 0 \\ & P_{Gi}^{\min} \leq P_{Gi} \leq P_{Gi}^{\max}, P_{Li}^{\min} \leq P_{Li} \leq P_{Li}^{\max} \end{aligned} \quad (5)$$

The incremental cost of participant i is defined as

$$w_i = 2\alpha_i P_{Gi} + \beta_i, \;\; or \;\; w_i = -2\sigma_i P_{Li} + \omega_i. \quad (6)$$

The well-known solution to (5) is the equal incremental cost criterion as introduced in [17], [26], and the proof is provided in Appendix I.

$$\begin{cases} w_i = w^*, & P_{Gi}^{\min} < P_{Gi} < P_{Gi}^{\max} \text{ or } P_{Li}^{\min} < P_{Li} < P_{Li}^{\max} \\ w_i \leq w^*, & P_{Gi} = P_{Gi}^{\max} \text{ or } P_{Li} = P_{Li}^{\max} \\ w_i \geq w^*, & P_{Gi} = P_{Gi}^{\min} \text{ or } P_{Li} = P_{Li}^{\min} \end{cases} \quad (7)$$

where w^* is the optimal equal incremental cost. As described in [27] and [28], the optimal solution of Eqn. (7) can be extended to any convex cost function.

The renewable energy generator is often controlled in maximum power point tracking mode, whose power output is subjected to weather conditions. Since the renewable energy generation is highly intermittent, energy storage system is utilized to smooth its output power fluctuation. Therefore, the combined output of renewable energy generator and energy storage system can be modeled as nondispatchable generation [4], which can be subtracted from the local load to calculate the local net load as in [28].

The key to solving the optimal energy management is to discover the optimal incremental cost, which will be discussed in the following section.

III. Proposed Distributed Optimal Algorithm

For simplicity, the incremental cost of generation or load demand $w_i(t)$ at time step t is denoted as state variable $x_i(t)$, and its adjusting rate $\dot{x}_i(t)$ is designed to be the linear combination of the current state and the control input. Thus, the dynamic behavior is given by

$$\dot{x}_i(t) = x_i(t) + u_i(t). \quad (8)$$

First, each unit does not have access to global information, and it discovers the common incremental cost using the consensus algorithm by minimizing the difference of the incremental between neighboring units.

Second, the adjustment rate should be controlled to optimize the process of generation or load changes. According to Eqn. (6), the generation or load demand is in linear relationship with the incremental cost $w_i(t)$, thus, Eqn. (8) can be rewritten as:

$$\dot{P}_{Gi}(t) = (w_i(t) + u_i(t)) \big/ 2\alpha_i \quad (9)$$

$$\text{Or} \quad \dot{P}_{Li}(t) = -(w_i(t) + u_i(t)) \big/ 2\sigma_i. \quad (10)$$

According to Eqn. (6), the incremental cost depends on the present generation or load which can be considered as uncontrollable value, therefore minimizing the control input can reduce the generation or load adjustment rate.

For simplicity, the desired final state is assumed to be zero at first, thus, the objective function is formulized as

$$\begin{aligned} J &= \sum_{i=1}^{n} J_i \\ &= \sum_{i=1}^{n} \Bigg\{ \frac{1}{2} s_i(T) x_i^2(T) + \int_{t_0}^{T} \Bigg(\frac{e}{2} \sum_{j \in N_i} \left[l_{ij}(x_i(t) - x_j(t)) \right]^2 \\ &\qquad \frac{m}{4} \sum_{j \in N_i} l_{ij} \left[x_i(t) - x_j(t) \right]^2 \\ &\qquad + \frac{1}{2} f x_i^2(t) + \frac{1}{2} r u_i^2(t) \Bigg) dt \Bigg\}. \\ &= \frac{1}{2} x^T(T) \mathbf{S}(T) x(T) \\ &\quad + \frac{1}{2} \int_{t_0}^{T} \left[x^T(t) \mathbf{Q} x(t) + u^T(t) \mathbf{R}(t) u(t) \right] dt \end{aligned} \quad (11)$$

$$\mathbf{Q} = e\mathbf{L}^2 + m\mathbf{L} + f\mathbf{I}_n \quad (12)$$

where T is the final time stamp, $s_i(T)$ is weight of the final state, $\mathbf{L}$ is defined in Appendix II, e, m, f, r are the weight coefficients, $\mathbf{R} = r\mathbf{I}_n$, and $\mathbf{S}(T) = diag(s_1(T), \cdots, s_n(T))$.

The designed optimal control law is distributed in nature (please refer to Appendix III for details), which is represented by

$$u_i(t) = -\sqrt{r^{-1}e}\sum_{j\in N_i} l_{ij}\left[x_i(t) - x_j(t)\right] - \left(1 + \frac{m}{2\sqrt{re}}\right)x_i(t). \tag{13}$$

Although the distributed control law is derived from the continuous form, it can also be implemented in discrete time for measurements are usually taken in discrete steps. Consider the communication topology may change from time to time, l_{ij} should be updated as $l_{ij}(k)$. Therefore, the distributed control law is modified as

$$u_i(k) = -\sqrt{r^{-1}e}\sum_{j\in N_i} l_{ij}(k)\ \left[x_i(k) - x_j(k)\right] - \left(1 + \frac{m}{2\sqrt{re}}\right)x_i(k). \tag{14}$$

The objective is to maximize the overall social welfare, i.e., enable all units to reach the common incremental cost. The reference of the desired state variable in the objective function (11) is assumed to be zero. However, it can be easily adjusted to converge to the optimal incremental cost by coordinate translation, which aims to minimize the difference of present incremental cost and the optimal incremental cost:

$$u_i(k) = -\sqrt{r^{-1}e}\sum_{j\in N_i} l_{ij}(k)\Big[\big(x_i(k) - w_i^*(k)\big) - \big(x_j(k) - w_j^*(k)\big)\Big] - \left(1 + \frac{m}{2\sqrt{re}}\right)\big(x_i(k) - w_i^*(k)\big). \tag{15}$$

According to [20], the optimal incremental cost can be discovered in a distributed way simultaneously as

$$w_i^*(k+1) = w_i^*(k) + \sum_{j\in N_i} l_{ij}(k)\Big[w_j^*(k) - w_i^*(k)\Big] + \varepsilon \cdot P_{Di}(k) \tag{16}$$

$$P_{Gi}(k+1) = \begin{cases} P_{Gi}^{\max}, & \dfrac{w_i^*(k+1) - \beta_i}{2\alpha_i} \geq P_{Gi}^{\max} \\ \dfrac{w_i^*(k+1) - \beta_i}{2\alpha_i}, & P_{Gi}^{\min} < \dfrac{w_i^*(k+1) - \beta_i}{2\alpha_i} < P_{Gi}^{\max} \\ P_{Gi}^{\min}, & \dfrac{w_i^*(k+1) - \beta_i}{2\alpha_i} \leq P_{Gi}^{\min} \end{cases} \tag{17}$$

or

$$P_{Li}(k+1) = \begin{cases} P_{Li}^{\max}, & \dfrac{w_i^*(k+1) - \omega_i}{-2\sigma_i} \geq P_{Li}^{\max} \\ \dfrac{w_i^*(k+1) - \omega_i}{-2\sigma_i}, & P_{Li}^{\min} < \dfrac{w_i^*(k+1) - \omega_i}{-2\sigma_i} < P_{Li}^{\max} \\ P_{Li}^{\min}, & \dfrac{w_i^*(k+1) - \omega_i}{-2\sigma_i} \leq P_{Li}^{\min} \end{cases} \tag{18}$$

$$P'_{Di}(k+1) = P_{Di}(k) + (P_{Gi}(k+1) - P_{Gi}(k)) \tag{19}$$

$$\text{or } P'_{Di}(k+1) = P_{Di}(k) + (P_{Li}(k+1) - P_{Li}(k)) \tag{20}$$

TABLE I
DISTRIBUTED OPTIMAL CONTROL BASED ENERGY MANAGEMENT

I. Initialization

t=0, Δt=2s, T=30s, $\epsilon = 0.02$, e=0.25 m=1, f=0, r =1;

$w_i(0) = 2\alpha_i P_{Gi}(0) + \beta_i$, or $w_i(0) = -2\sigma_i P_{Li}(0) + \omega_i$

$P'_{Di}(0) = P_{Gi}(0)$ or $P'_{Di}(0) = P_{Li}(0)$

II. Distributed optimal control algorithm

while $t<T$ (%T is the time interval for local power measurement update)

Each unit communicates with neighboring agents through a peer-to-peer communication network based on the updating rules of Eqns. (16)-(21);

Each unit updates the control variable according to Eqn. (15);

Each unit adjusts its generation output or load demand based on the control signal;

t=t+Δt;

End

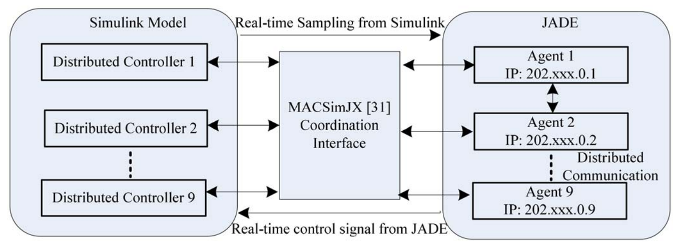

Fig. 1. Schematic diagram of the communication between JADE and Simulink model.

$$P_{Di}(k+1) = P'_{Di}(k+1) + \sum_{j\in N_i} l_{ij}(k)\Big(P'_{Dj}(k+1) - P'_{Di}(k+1)\Big) \tag{21}$$

where ε is the step size, $P'_{Di}(k+1)$ is the local estimated supply-demand mismatch, $P_{Di}(k+1)$ is the updated global supply-demand mismatch.

Note that the proposed distributed control algorithm only requires local and neighborhood information (i.e., incremental cost, optimal incremental cost, local estimated supply-demand mismatch) to update the control law, no global parameter of the system is required, and it is adaptive to topology changes. The step-by-step procedure of the proposed algorithm is shown in Table I.

IV. SIMULATION STUDIES

In this section, four case studies are presented to exhibit the effectiveness of the proposed distributed algorithm for maintaining the generation-demand balance in power grids. Case study 1 demonstrates the performance of the proposed algorithm on the IEEE 9-bus system with ideal communication network as shown in Fig. 2, whereas case study 2 is carried out to investigate its robustness against communication failure. A 9-bus system test-bed is built in Matlab/Simulink, and the parameters of three generators are provided in Appendix IV. The agent-based control system is developed using Java agent development (JADE) platform. The communication between JADE and Simulink is realized using MACSimJX interface [31], which is shown in Fig. 1. The 9-bus system is connected to the main grid with capacity of 1000MVA. Each unit updates its generation or load for every two seconds according to the proposed algorithm

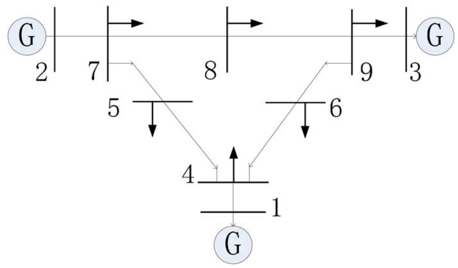

Fig. 2. Topology of the IEEE 9-bus system.

TABLE II
COST COEFFICIENTS FOR NINE UNITS

Generator	α_i	β_i	P_{Gi}^{min}	P_{Gi}^{max}	$P_{Gi}[0]$
1	0.080	2.25	30 MW	70 MW	60 MW
2	0.062	4.20	20 MW	65 MW	45 MW
3	0.075	3.25	20 MW	70 MW	55 MW
Load	σ_i	ω_i	P_{Li}^{min}	P_{Li}^{max}	$P_{Li}[0]$
4	0.072	8.25	20 MW	50 MW	20 MW
5	0.066	7.90	30 MW	60 MW	40 MW
6	0.070	7.55	10 MW	30 MW	15 MW
7	0.055	8.00	15 MW	40 MW	25 MW
8	0.075	7.75	10 MW	40 MW	30 MW
9	0.045	8.05	30 MW	70 MW	45 MW

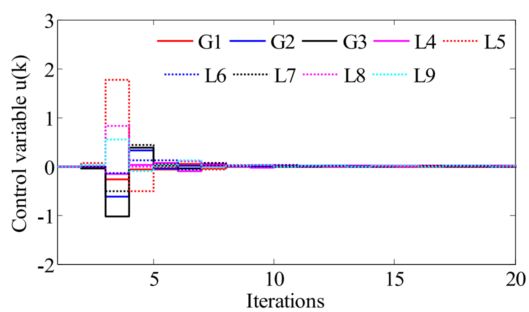

Fig. 3. Control variable update with ideal communication network.

in Table I. Case study 3 demonstrates the adaptivity of the proposed algorithm to the system topology changes. The scalability of the proposed algorithm is validated through the test on a 200-unit system in case study 4.

A. Case Study 1: IEEE 9-Bus System With Ideal Communication Network

In this case, the communication topology of all units is assumed to be the same as the IEEE 9-bus system network, which implies that two units can exchange information if there is a physical power line connection between them. There are three generation units and six load units in the system, whose parameters are provided in Table II, and the step size of ϵ in Eqn. (16) is set to 0.02 by trial and error, weight coefficients e, m, f, and r are set to 1/4, 1, 0, 1, respectively.

It is assumed that the system is disturbed at the first iteration by sudden generation/load changes, and the proposed distributed algorithm is applied to restore the power balance in an optimal way. The updates of the control variable, generation-demand, local incremental cost and the mismatch estimation of each participant under an ideal communication network are shown in Figs. 3-6.

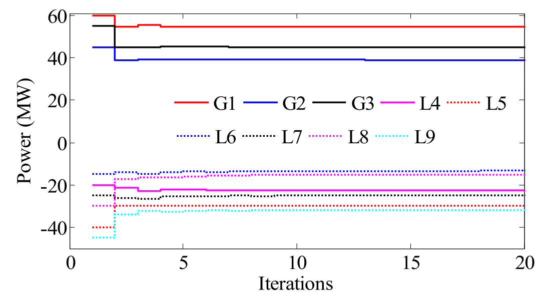

Fig. 4. Local supply/demand update with ideal communication network.

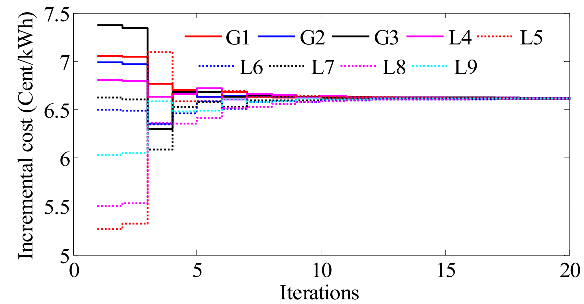

Fig. 5. Incremental cost update with ideal communication network.

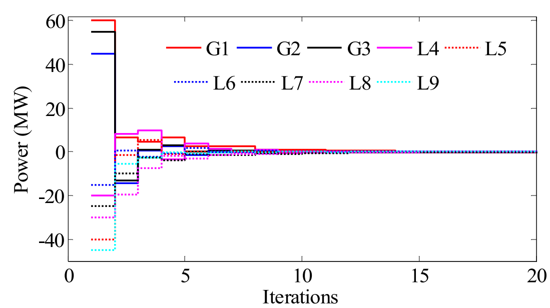

Fig. 6. Local supply-demand mismatch estimation update with ideal communication network.

In Fig. 3, the control variable is less than 2MW/iteration, which can be adjusted by tuning the parameter of r. Larger value of r can be chosen if generator adjustment rate is weighed as a more important factor. In Fig. 4, the minimum load demand of unit 6 is -10MW, and it is kept within its boundary under the proposed distributed control algorithm. The incremental cost converges to a common value w^* within 10 iterations and the supply-demand balance converges to zero, as shown in Figs. 5 and 6, respectively. The global generation-demand mismatch diminishes very fast, from initial value -15MW to -5MW at the first iteration, and then gradually goes to zero as shown in Fig. 7.

In real-time implementation, the sampling time interval of the communication is chosen to be 2s, considering both the response time of generators and the time interval for distributed controller data exchange. The time consumed by a message to be sent between two agents is quite short. The average time is found to be 0.034s in the real-time implementation, which mainly depends on the hardware (different computers), software implementation (coding, compliers) and distance [32].

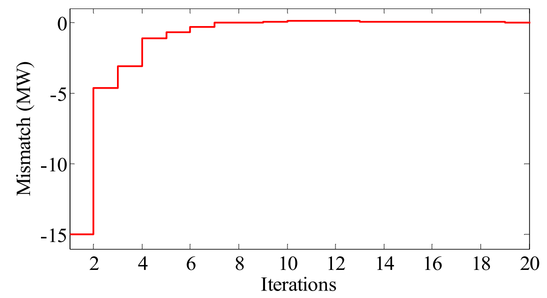

Fig. 7. Global supply-demand mismatch profile with ideal communication network.

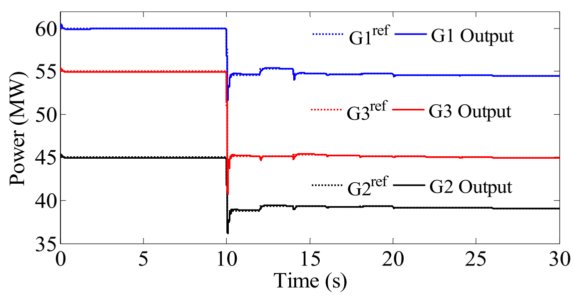

Fig. 8. Active power output tracking profile of generators.

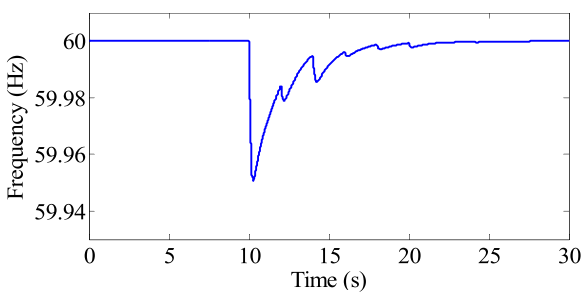

Fig. 9. System frequency profile with ideal communication network.

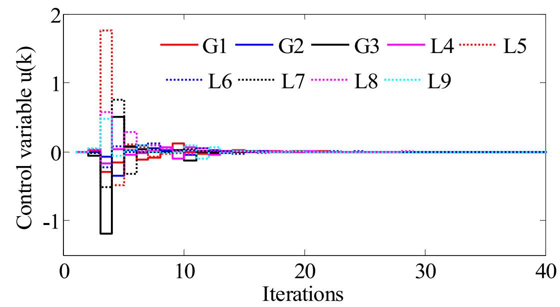

Fig. 10. Control variable update under communication failure.

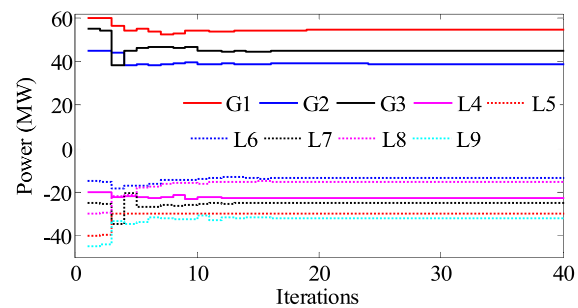

Fig. 11. Local supply/demand update under communication failure.

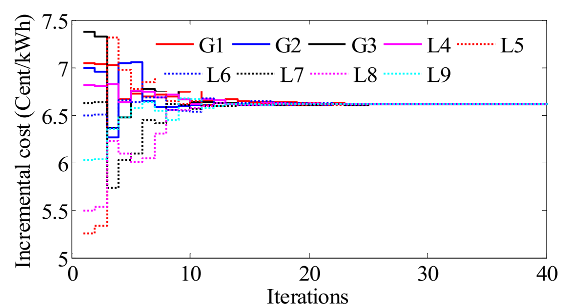

Fig. 12. Incremental cost update under communication failure.

The system is disturbed at the time instant of 10s, which is caused by sudden generation/load changes. The proposed distributed algorithm is triggered to restore the system supply-demand balance. As shown in Fig. 8, the generator active power output is able to track the reference within 0.5s for each control cycle of 2s. The system frequency is able to stabilize within 10s, with maximum deviation of 0.05 Hz when the supply-demand imbalance is the greatest. The smaller deviation peaks occur at the start of each control cycle are caused by the generator tracking dynamic, as shown in Fig. 9.

B. Case Study 2: IEEE 9-Bus System Under Communication Failure

In real application, communication network is usually imperfect, and this study case investigates the robustness of the proposed distributed algorithm against communication failure. In this case, the communication failure probability is deliberately set to a large value of 0.3 to consider the worst scenario. It is simulated by introducing a random number ranges from zero to one at each iteration for each communication channel. If the random number is less than or equal to 0.3, then the communication coefficient l_{ij} is set to zero, if the random number is larger than 0.3, then l_{ij} is set as in Eqn. (23). Note that, each agent at least requires one communication channel available during the updating process in worst case scenario.

Figs. 10-14 show the updates of the control variable, generation-demand, local incremental cost, the local mismatch estimation and the global supply-demand mismatch under communication failure. The proposed distributed optimal control algorithm is no longer globally optimal in imperfect communication network, which will take longer time to converge.

The system frequency dynamic performance is shown in Fig. 15, which is able to stabilize within 20s with a maximum deviation of 0.09Hz. The simulation results have demonstrated the proposed algorithm can achieve almost the same optimal solution to the case under an ideal communication network with longer time. Thus, the proposed algorithm is robust to communication failures.

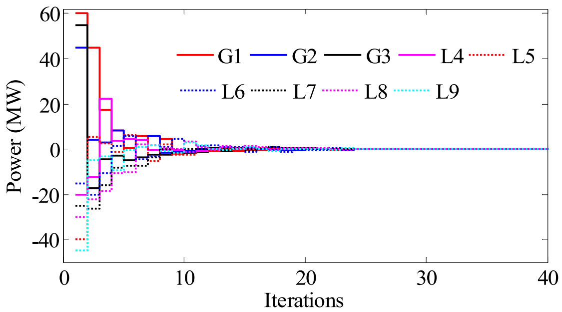

Fig. 13. Local supply-demand mismatch estimation update under communication failure.

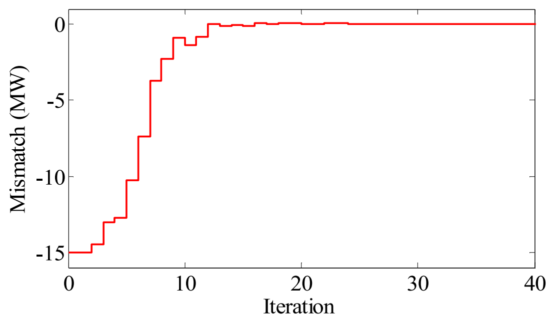

Fig. 14. Global supply-demand mismatch update under communication failure.

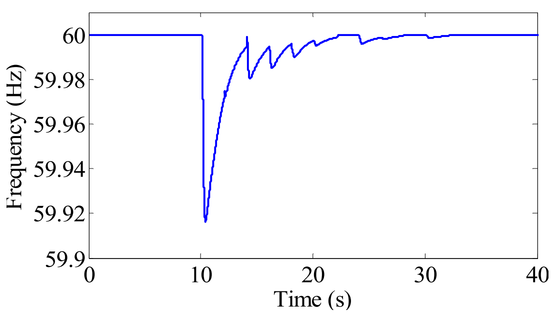

Fig. 15. System frequency profile under communication failure.

C. Case Study 3: IEEE 39-Bus System

This study case investigates the performance of the proposed distributed algorithm by testing with the IEEE 39-bus system under system topology changes. The communication network is also assumed to be the same as the physical network in this case. There are 10 generation units and 29 load units, and the parameters of the cost function are listed in Table III. The simulation starts with 39 units, however, at the 100th iteration, load units 5, 6, 8, 12 and 24 are switched off, then they rejoin again at the 200th iteration.

The simulation results of the updates of the control variable, generation-demand, local incremental cost, local supply-demand mismatch estimation, and global supply-demand mismatch under topology changes are shown in Figs. 16-20. For larger system, the proposed distributed algorithm takes more iterations to converge, about 50 iterations for the 39-unit system, which implies that iteration number does not increase exponentially with the size of the system.

TABLE III
COST COEFFICIENTS FOR 39 UNITS

Load	σ_i	ω_i	Load	σ_i	ω_i
1	0.078	8.25	2	0.058	7.90
3	0.073	8.23	4	0.051	7.92
5	0.070	8.84	6	0.055	7.21
7	0.075	7.27	8	0.054	9.01
9	0.051	8.27	10	0.067	7.95
11	0.065	7.85	12	0.062	7.88
13	0.058	8.12	14	0.061	8.85
15	0.054	8.45	16	0.064	8.33
17	0.069	8.21	18	0.077	8.17
19	0.081	8.07	20	0.079	8.53
21	0.049	8.06	22	0.052	8.11
23	0.053	8.22	24	0.059	8.09
25	0.066	7.99	26	0.069	7.87
27	0.073	7.77	28	0.074	7.79
29	0.075	8.43			
Generator	α_i	β_i	Generator	α_i	β_i
30	0.055	3.56	31	0.042	3.45
32	0.043	4.25	33	0.044	3.65
34	0.052	4.15	35	0.069	4.50
36	0.048	4.05	37	0.050	4.13
38	0.063	2.75	39	0.076	2.91

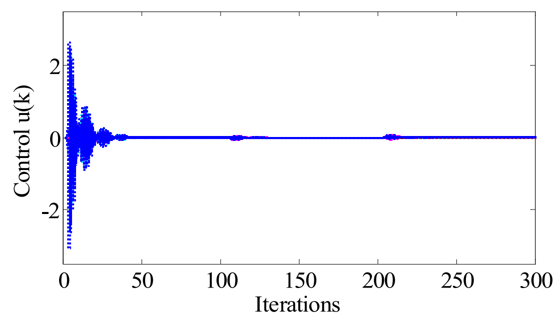

Fig. 16. Control variable update under topology changes.

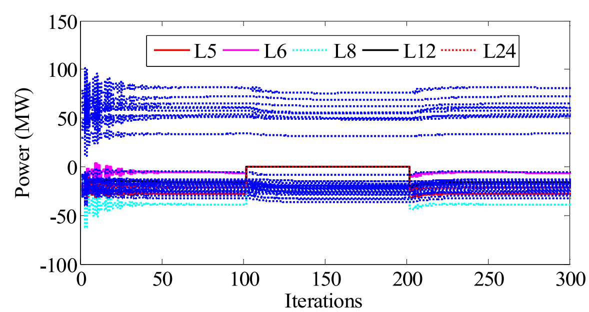

Fig. 17. Local supply/demand update under topology changes.

At the 100th iteration, when several load units are switched off, the system topology changes, the communication coefficients can be updated automatically according to Eqn. (23), which only require updating the existing number of neighbors for each unit. Similarly, at the 200th iteration, when the load units rejoin the process, the communication coefficients can be updated in a timely manner.

As shown in Figs. 17 and 18, at the 100th iteration, the available generation is more than the present demand, the incremental cost decreases, thus the rest load units can use more power while the generation units tend to decrease the supply until they reach a new balance. Similarly, when the load

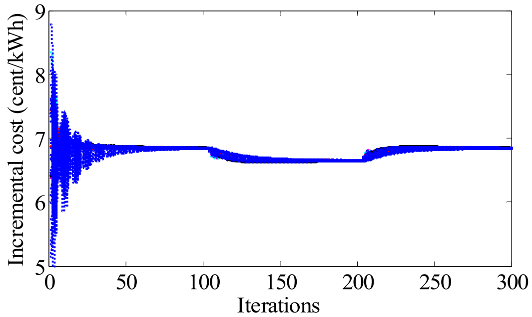

Fig. 18. Incremental cost update under topology changes.

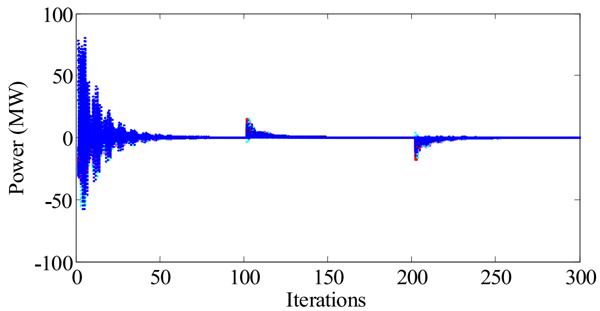

Fig. 19. Local supply-demand mismatch estimation update under topology changes.

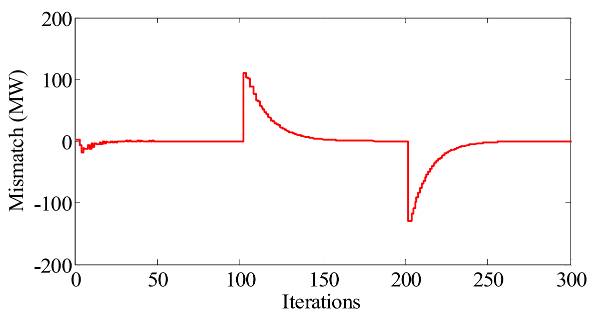

Fig. 20. Global supply-demand mismatch estimation update under topology changes.

units rejoin the process, the available generation is less than the present load demand, the incremental cost increases, the load units would use less power while the generation units are willing to supply more power. During the dynamic process of units' plug and play, the proposed algorithm enables the incremental costs of all units converge to the common value and the generation-demand mismatches converge to zero, as shown in Figs. 18-20, which demonstrates its adaptivity against topology changes.

D. Case Study 4: 200-Unit System

This study case investigates the scalability of the proposed distributed algorithm by testing with a 200-unit system, with 100 generation units and 100 load units. The adopted network is designed by assuming unit i is connected with its adjacent 20 neighbors in the order of index number of $i-10, \ldots, i-1$, and $i+1, \ldots, i+10$.

The simulation results of the updates of the control variable and the mismatch estimation of each participant are

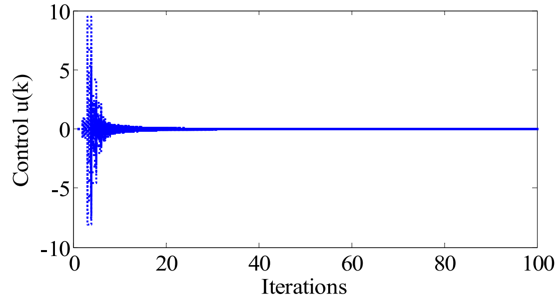

Fig. 21. Control variable update for 200-unit system.

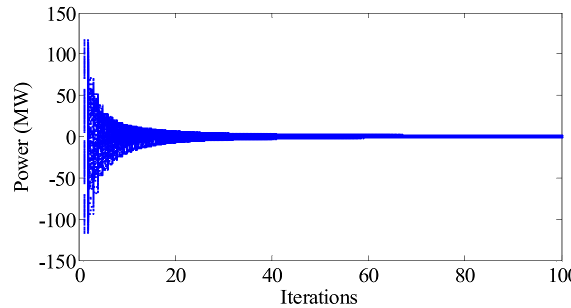

Fig. 22. Supply-demand mismatch estimation update for 200-unit system.

shown in Figs. 21-22. The proposed approach converges within 80 iterations for the 200-unit system, which indicates the converging speed is not only associated with the number of units but also the connectivity of the communication network. Thus, with a properly designed communication network, the proposed algorithm can converge in a timely manner, which indicates its promising application in large complicated systems.

V. Conclusion

The proposed real-time distributed optimal control based algorithm depends on only local computation and sparse communication network, which renders a more viable solution. The proposed distributed algorithm converges to the global optimal incremental cost for all participants to maximize the overall social welfare, while maintaining the generation-demand balance and considering the adjustment rate in the dynamic process. As demonstrated in the simulations, the proposed distributed algorithm is robust to communication failures, adaptive to communication topology changes, and scalable to large systems. The major advantage of the proposed distributed algorithm is to minimize the impact of dynamic adjustments to the system frequency as validated in the real-time simulation. Thus, the proposed distributed algorithm shows its promising application in practical systems.

It should be noted that the combined output of renewable energy generator and the energy storage system is still stochastic, thus an online algorithm developed in [28] would be helpful to address the stochastic nature. The future work is to refine the distributed solutions, such as introducing energy storage system constraints and realizing real-time implementation in a distributed fashion.

APPENDIX I: PROOF OF EQN. (7)

Formula (5) is a maximization problem which is equivalent to

$$\begin{aligned} \text{Minimize} \quad & \sum_{i=1}^{n} C_i(P_{Gi}) - \sum_{i=1}^{n} D_i(P_{Li}) \\ \text{s.t.} \quad & \sum_{i=1}^{n} P_{Gi} - \sum_{i=1}^{n} P_{Li} = 0 \\ & P_{Gi}^{\min} \le P_{Gi} \le P_{Gi}^{\max}, P_{Li}^{\min} \le P_{Li} \le P_{Li}^{\max}. \end{aligned} \tag{22}$$

The Lagrange function for the optimization problem (22) is given by

$$\begin{aligned} L = & \sum_{i=1}^{n} C_i(P_{Gi}) - \sum_{i=1}^{n} D_i(P_{Li}) + w\left(\sum_{i=1}^{n} P_{Li} - \sum_{i=1}^{n} P_{Gi}\right) \\ & + \sum_{i=1}^{n} \mu_{Pi}^{+}\left(P_{Gi} - P_{Gi}^{\max}\right) + \sum_{i=1}^{n} \mu_{Pi}^{-}\left(-P_{Gi} + P_{Gi}^{\min}\right) \\ & + \sum_{i=1}^{n} \mu_{Li}^{+}\left(P_{Li} - P_{Li}^{\max}\right) + \sum_{i=1}^{n} \mu_{Li}^{-}\left(-P_{Li} + P_{Li}^{\min}\right) \end{aligned} \tag{23}$$

where w and $\mu_{Pi}^{+}, \mu_{Pi}^{-}, \mu_{Li}^{+}, \mu_{Li}^{-} \ge 0$ correspond to Lagrange multipliers. Hence, the first order optimality conditions result in

$$\frac{\partial L}{\partial P_{Gi}} = 2\alpha_i P_{Gi} + \beta_i + \mu_{Pi}^{+} - \mu_{Pi}^{-} - w = 0 \tag{24.a}$$

$$\frac{\partial L}{\partial P_{Li}} = -2\sigma_i P_{Li} + \omega_i + \mu_{Li}^{+} - \mu_{Li}^{-} + w = 0 \tag{24.b}$$

$$\frac{\partial L}{\partial w} = \sum_{i=1}^{n} P_{Li} - \sum_{i=1}^{n} P_{Gi} = 0 \tag{24.c}$$

$$\frac{\partial L}{\partial \mu_{Gi}^{+}} = P_{Gi} - P_{Gi}^{\max} \le 0 \tag{24.d}$$

$$\frac{\partial L}{\partial \mu_{Gi}^{-}} = P_{Gi}^{\min} - P_{Gi} \le 0 \tag{24.e}$$

$$\frac{\partial L}{\partial \mu_{Li}^{+}} = P_{Li} - P_{Li}^{\max} \le 0 \tag{24.f}$$

$$\frac{\partial L}{\partial \mu_{Li}^{-}} = P_{Li}^{\min} - P_{Li} \le 0 \tag{24.g}$$

$$\mu_{Gi}^{+}\frac{\partial L}{\partial \mu_{Gi}^{+}} = \mu_{Gi}^{+}\left(P_{Gi} - P_{Gi}^{\max}\right) = 0 \tag{24.h}$$

$$\mu_{Gi}^{-}\frac{\partial L}{\partial \mu_{Gi}^{-}} = \mu_{Gi}^{-}\left(P_{Gi}^{\min} - P_{Gi}\right) = 0 \tag{24.i}$$

$$\mu_{Li}^{+}\frac{\partial L}{\partial \mu_{Li}^{+}} = \mu_{Li}^{+}\left(P_{Li} - P_{Li}^{\max}\right) = 0 \tag{24.j}$$

$$\mu_{Gi}^{-}\frac{\partial L}{\partial \mu_{Gi}^{-}} = \mu_{Gi}^{-}\left(P_{Gi}^{\min} - P_{Gi}\right) = 0. \tag{24.k}$$

If $P_{Gi}^{\min} < P_{Gi} < P_{Gi}^{\max}$, according to (24. h) and (24. i), it yields $\mu_{Gi}^{+}, \mu_{Gi}^{-} = 0$. Then, according to (24. a),

$$w^{*} = 2\alpha_i P_{Gi} + \beta_i = w_i. \tag{24.l}$$

If $P_{Gi} = P_{Gi}^{\max}$, according to (24. h) and (24. i), $P_{Gi} - P_{Gi}^{\max} = 0$, $P_{Gi}^{\min} - P_{Gi} < 0$. Therefore, we have μ_{Gi}^{+}=0, $\mu_{Gi}^{-} \ge 0$. Then, according to (24. a), it yields:

$$w^{*} = 2\alpha_i P_{Gi}^{\max} + \beta_i + \mu_{Gi}^{-} \ge 2\alpha_i P_{Gi}^{\max} + \beta_i = w_i. \tag{24.m}$$

If $P_{Gi} = P_{Gi}^{\min}$, according to (24. h) and (24. i), $P_{Gi} - P_{Gi}^{\max} < 0$, $P_{Gi}^{\min} - P_{Gi} = 0$. Thus, $\mu_{Gi}^{+} \ge 0, \mu_{Gi}^{-} = 0$. Then, according to (24. a),

$$w^{*} = 2\alpha_i P_{Gi}^{\min} + \beta_i - \mu_{Gi}^{+} \le 2\alpha_i P_{Gi}^{\min} + \beta_i = w_i. \tag{24.n}$$

Similar relationship of P_{Li} and w^{*} can be derived. Combine situations of (24.l-24.n), it yields Eqn. (7).

APPENDIX II: CONSENSUS ALGORITHM

According to the consensus algorithm, the information updating process is represented as

$$\dot{x}_i(t) = \sum_{j=1}^{n} l_{ij}\left[x_i(t) - x_j(t)\right], \quad i = 1, \cdots, n. \tag{25}$$

where x_i are the local information discovered by node i, l_{ij} is the communication coefficient between node i and j, and n is the number of total nodes.

Different methods for l_{ij} determination provide different converging speeds. The *mean metropolis* algorithm introduced in [29] is distributed, adaptive to changes of communication network topology, thus, it is adopted in this paper.

$$l_{ij} = \begin{cases} -2/\left(n_i + n_j + 1\right) & j \in N_i \\ \sum_{j \in N_i} 2/\left(n_i + n_j + 1\right) & i = j \\ 0 & otherwise \end{cases} \tag{26}$$

where n_i and n_j are the numbers of nodes connected to node i and j, respectively.

APPENDIX III: DISTRIBUTED OPTIMAL CONTROL ALGORITHM

The dynamic behavior of multi-unit system is represented in a matrix form as

$$\dot{x}(t) = \mathbf{A}x(t) + \mathbf{B}u(t). \tag{27}$$

where $x(t) = [x_1(t), \cdots, x_n(t)]^T$, $u(t) = [u_1(t), \cdots, u_n(t)]^T$, $\mathbf{A}$ and $\mathbf{B}$ are n-dimensional identity matrix $\mathbf{I}_n$.

To solve the linear quadratic regulator (LQR) problem formulated in Eqn. (11), the Hamilton function is defined as

$$H = \frac{1}{2}\left(x^T(t)\mathbf{Q}x(t) + u^T(t)\mathbf{R}u(t)\right) + \lambda^T(t)(\mathbf{A}x(t) + \mathbf{B}u(t)) \tag{28}$$

where $\lambda(t)$ is a vector of the Lagrange-multipliers at time t.

The state and co-state equations and the stationary condition are given as follows

$$\dot{x}(t) = \frac{\partial H}{\partial \lambda(t)} = \mathbf{A}x(t) + \mathbf{B}u(t). \tag{29}$$

$$-\dot{\lambda}(t) = \frac{\partial H}{\partial x(t)} = \mathbf{Q}x(t) + \mathbf{A}^T\lambda(t). \tag{30}$$

$$0 = \frac{\partial H}{\partial u(t)} = \mathbf{R}u(t) + \mathbf{B}^T\lambda(t). \tag{31}$$

According to Eqn. (31), the control variable $u(t)$ can be determined as

$$u(t) = -\mathbf{R}^{-1}\mathbf{B}\lambda(t). \tag{32}$$

Substitute Eqn. (32) into Eqn. (29) and (30), the state and co-state equations become

$$\dot{x}(t) = \mathbf{A}x(t) - \mathbf{B}\mathbf{R}^{-1}\mathbf{B}^T\lambda(t) \tag{33}$$

$$\dot{\lambda}(t) = -\mathbf{Q}x(t) - \mathbf{A}^T\lambda(t) \tag{34}$$

The boundary condition is given by

$$\lambda(T) = \frac{\partial\left(x^T(T)\mathbf{S}(T)x(T)/2\right)}{\partial x(T)} = \mathbf{S}(T)x(T). \tag{35}$$

Sweep method [30] is introduced to solve Eqn. (35) by assuming a linear relation holds for all $t_0 \leq t \leq T$

$$\lambda(t) = \mathbf{S}(t)x(t). \tag{36}$$

Take the derivative with respect to t on both sides of Eqn. (36), yields

$$\dot{\lambda}(t) = \dot{\mathbf{S}}(t)x(t) + \mathbf{S}(t)\dot{x}(t). \tag{37}$$

Substitute Eqn. (33), (34) and (36), Eqn. (39) becomes

$$\begin{aligned} &\dot{\mathbf{S}}(t)x(t) + \mathbf{S}(t)(\mathbf{A}x(t) - \mathbf{B}\mathbf{R}^{-1}\mathbf{B}^T\mathbf{S}(t)x(t)) \\ &\quad = -\mathbf{Q}x(t) - \mathbf{A}^T\mathbf{S}(t)x(t) \end{aligned} \tag{38}$$

Eqn. (38) is valid for all $x(t)$ which is usually nonzero, thus

$$-\dot{\mathbf{S}}(t) = \mathbf{A}^T\mathbf{S}(t) + \mathbf{S}(t)\mathbf{A} - \mathbf{S}(t)\mathbf{B}\mathbf{R}^{-1}\mathbf{B}^T\mathbf{S}(t) + \mathbf{Q}. \tag{39}$$

When $\mathbf{S}(t)$ converges, evidently $\dot{\mathbf{S}}(t) = 0$, Eqn. (39) becomes

$$\mathbf{A}^T\mathbf{S}(t) + \mathbf{S}(t)\mathbf{A} - \mathbf{S}(t)\mathbf{B}\mathbf{R}^{-1}(k)\mathbf{B}^T\mathbf{S}(t) + \mathbf{Q} = 0. \tag{40}$$

Substitute $\mathbf{A}$ and $\mathbf{B}$ as identity matrix in Eqn. (40), yields

$$\mathbf{R}^{-1}\mathbf{S}^2(t) - 2\mathbf{S} - \mathbf{Q} = 0. \tag{41}$$

Premultiply $\mathbf{R}^{-1}$ on both sides of Eqn. (41) becomes

$$\left(\mathbf{R}^{-1}\right)^2\mathbf{S}^2(t) - 2\mathbf{R}^{-1}\mathbf{S}(t) - \mathbf{R}^{-1}\mathbf{Q} = 0. \tag{42}$$

Eqn. (42) is then rewritten as

$$\left(\mathbf{R}^{-1}\mathbf{S}(t) - \mathbf{I}_n\right)^2 = \mathbf{R}^{-1}\mathbf{Q} + \mathbf{I}_n. \tag{43}$$

The term $\mathbf{R}^{-1}\mathbf{S}(t)$ which is essential to determine the control input is calculated as

$$\mathbf{R}^{-1}\mathbf{S}(t) = \mathbf{I}_n + \sqrt{\mathbf{R}^{-1}\mathbf{Q} + \mathbf{I}_n}. \tag{44}$$

The second term on the R.H.S of Eqn. (44) is expanded by substituting $\mathbf{R}^{-1}$ and $\mathbf{Q}$

$$\sqrt{\mathbf{R}^{-1}\mathbf{Q} + \mathbf{I}_n} = \sqrt{r^{-1}}\sqrt{e\mathbf{L}^2 + m\mathbf{L} + r\mathbf{I}_n + f\mathbf{I}_n}. \tag{45}$$

The second term on the R.H.S of Eqn. (45) becomes a perfect square term if the following relationship of m, f, e, r holds

$$m^2 - 4e(f + r) = 0. \tag{46}$$

Thus, f is designed as

$$f = \frac{m^2}{4e} - r. \tag{47}$$

Substitute Eqn. (47) in Eqn. (45), yields

$$\begin{aligned} &\sqrt{r^{-1}}\sqrt{e\mathbf{L}^2 + m\mathbf{L} + r\mathbf{I}_n + \left(\frac{m^2}{4e} - r\right)\mathbf{I}_n} \\ &\qquad = \sqrt{r^{-1}}\sqrt{\left(\sqrt{e}\mathbf{L} + \frac{m}{2\sqrt{e}}\right)^2}. \end{aligned} \tag{48}$$

Therefore, the term of $\mathbf{R}^{-1}\mathbf{S}(t)$ is now determined by

$$\mathbf{R}^{-1}\mathbf{S}(t) = \sqrt{r^{-1}}e\mathbf{L} + \left(1 + \frac{m\sqrt{r^{-1}}}{2\sqrt{e}}\right)\mathbf{I}_n. \tag{49}$$

According to Eqn. (32) and (36), the optimal control law is represented by

$$u(t) = -\mathbf{R}^{-1}\mathbf{B}\lambda(t) = -\mathbf{R}^{-1}\mathbf{S}(t)x(t). \tag{50}$$

Substitute Eqn. (49) in Eqn. (50), the optimal control law becomes

$$u(t) = -\left(\sqrt{r^{-1}}e\mathbf{L} + \left(1 + \frac{m}{2\sqrt{re}}\right)\mathbf{I}_n\right)x(t). \tag{51}$$

Since $\mathbf{L}$ is the Laplacian matrix, the designed optimal control law is distributed in nature, which is represented by

$$u_i(t) = -\sqrt{r^{-1}}e\sum_{j\in N_i} l_{ij}\left[x_i(t) - x_j(t)\right] - \left(1 + \frac{m}{2\sqrt{re}}\right)x_i(t). \tag{52}$$

Appendix IV: Generator Parameters for 9-bus System

The parameters of the three generators are:

Generator 1: S_{base}=70 MW, H=3.5s, x_d=2.9 p.u., x_q=2.3 p.u., x'_d=0.58 p.u., x'_q=0.55 p.u., T'_{d0}=5.8 s, T'_{q0}=0.35 s;

Generator 2: S_{base}=65 MW, H=3.4s, x_d=2.9 p.u., x_q=2.7 p.u., x'_d=0.49 p.u., x'_q=0.51 p.u., T'_{d0}=5.7 s, T'_{q0}=0.38 s;

Generator 3: S_{base}=70 MW, H=3.6s, x_d=3.0 p.u., x_q=2.5 p.u., x'_d=0.65 p.u., x'_q=0.63 p.u., T'_{d0}=6.2s, T'_{q0}=0.42 s;

References

[1] A. Bose, "Smart transmission grid applications and their supporting infrastructure," *IEEE Trans. Smart Grid*, vol. 1, no. 1, pp. 11–19, Jun. 2010.

[2] V. C. Gungor *et al.*, "Smart grid technologies: Communication technologies and standards," *IEEE Trans. Ind. Informat.*, vol. 7, no. 4, pp. 529–539, Nov. 2011.

[3] X. Fang, S. Misra, G. Xue, and D. Yang, "Smart grid—The new and improved power grid: A survey," *IEEE Commun. Surveys Tuts.*, vol. 14, no. 4, pp. 944–980, Dec. 2012.

[4] I. Atzeni, L. G. Ordonez, G. Scutari, D. P. Palomar, and J. R. Fonollosa, "Noncooperative and cooperative optimization of distributed energy generation and storage in the demand-side of the smart grid," *IEEE Trans. Signal Process.*, vol. 61, no. 10, pp. 2454–2472, May 2013.

[5] T. Sadamoto, T. Ishizaki, M. Koike, Y. Ueda, and J.-I. Imura, "Spatiotemporally multiresolutional optimization toward supply–demand–storage balancing under PV prediction uncertainty," *IEEE Trans. Smart Grid*, vol. 6, no. 2, pp. 853–865, Mar. 2015.

[6] M. R. V. Moghadam, R. T. B. Ma, and Z. Rui, "Distributed frequency control in smart grids via randomized demand response," *IEEE Trans. Smart Grid*, vol. 5, no. 6, pp. 2798–2809, Nov. 2014.

[7] Y. Xu, W. Liu, and J. Gong, "Stable multi-agent based load shedding algorithm for power systems," *IEEE Trans. Power Syst.*, vol. 26, no. 4, pp. 2006–2014, Nov. 2011.

[8] Z. Zhang and M.-Y. Chow, "Convergence analysis of the incremental cost consensus algorithm under different communication network topologies in a smart grid," *IEEE Trans. Power Syst.*, vol. 27, no. 4, pp. 1761–1768, Nov. 2012.

[9] G. Binetti, A. Davoudi, F. L. Lewis, D. Naso, and B. Turchiano, "Distributed consensus-based economic dispatch with transmission losses," *IEEE Trans. Power Syst.*, vol. 29, no. 4, pp. 1711–1720, Jul. 2014.

[10] Y. Xu *et al.*, "Distributed subgradient-based coordination of multiple renewable generators in a microgrid," *IEEE Trans. Power Syst.*, vol. 29, no. 1, pp. 23–33, Jan. 2014.

[11] H. Xin, Z. Qu, J. Seuss, and A. Maknouninejad, "A self-organizing strategy for power flow control of photovoltaic generators in a distribution network," *IEEE Trans. Power Syst.*, vol. 26, no. 3, pp. 1462–1473, Aug. 2011.

[12] Y. M. Ding, S. H. Hong, and X. H. Li, "A demand response energy management scheme for industrial facilities in smart grid," *IEEE Trans. Ind. Informat.*, vol. 10, no. 4, pp. 2257–2269, Nov. 2014.

[13] M. Yazdanian and A. Mehrizi-Sani, "Distributed control techniques in microgrids," *IEEE Trans. Smart Grid*, vol. 5, no. 6, pp. 2901–2909, Nov. 2014.

[14] A. Chaouachi, R. M. Kamel, R. Andoulsi, and K. Nagasaka, "Multiobjective intelligent energy management for a microgrid," *IEEE Trans. Ind. Electron.*, vol. 60, no. 4, pp.1688–1699, Apr. 2013.

[15] A. Safdarian, M. Fotuhi-Firuzabad, and M. Lehtonen, "A distributed algorithm for managing residential demand response in smart grids," *IEEE Trans. Ind. Informat.*, vol. 10, no. 4, pp. 2385–2393, Nov. 2014.

[16] L. Zheng and C. Lin, "A distributed demand response control strategy using Lyapunov optimization," *IEEE Trans. Smart Grid*, vol. 5, no. 4, pp. 2075–2083, Jul. 2014.

[17] S. Yang, S. Tan, and J. Xu, "Consensus based approach for economic dispatch problem in a smart grid," *IEEE Trans. Power Syst.*, vol. 28, no. 4, pp. 4416–4426, Nov. 2013.

[18] R. Deng, Z. Yang, F. Hou, M.-Y. Chow, and J. Chen, "Distributed realtime demand response in multiseller–multibuyer smart distribution grid," *IEEE Trans. Power Syst.*, vol. 30, no. 5, pp. 2364–2374, Sep. 2015.

[19] N. Rahbari-Asr, U. Ojha, U. Z. Zhang, and M.-Y. Chow, "Incremental welfare consensus algorithm for cooperative distributed generation/demand response in smart grid," *IEEE Trans. Smart Grid*, vol. 5, no. 6, pp. 2836–2845, Nov. 2014.

[20] Y. Xu and Z. Li, "Distributed optimal resource management based on consensus algorithm in a microgrid," *IEEE Trans. Ind. Electron.*, vol. 62, no. 4, pp. 2584–2592, Apr. 2015.

[21] C. Wang and S. M. Shahidehpour, "Effects of ramp-rate limits on unit commitment and economic dispatch," *IEEE Trans. Power Syst.*, vol. 8, no. 3, pp. 1341–1350, Aug. 1993.

[22] F. N. Lee, L. Lemonidis, and K. Liu, "Price-based ramp-rate model for dynamic dispatch and unit commitment," *IEEE Trans. Power Syst.*, vol. 9, no. 3, pp. 1233–1242, Aug. 1994.

[23] M. Fahrioglu and F. L. Alvarado, "Using utility information to calibrate customer demand management behavior models," *IEEE Trans. Power Syst.*, vol. 16, no. 2, pp. 317–322, May 2001.

[24] Z. Fan, "A distributed demand response algorithm and its application to PHEV charging in smart grids," *IEEE Trans. Smart Grid*, vol. 3, no. 3, pp. 1280–1290, Sep. 2012.

[25] P. Samadi, H. Mohsenian-Rad, R. Schober, and V. W. S. Wong, "Advanced demand side management for the future smart grid using mechanism design," *IEEE Trans. Smart Grid*, vol. 3, no. 3, pp. 1170–1180, Sep. 2012.

[26] A. J. Wood and B. F. Wollenberg, *Power Generation, Operation, and Control*, 2nd ed. Hoboken, NJ, USA: Wiley, 1996, pp. 32–33.

[27] Y. Xu, "Optimal distributed charging rate control of plug-in electric vehicles for demand management," *IEEE Trans. Power Syst.*, vol. 30, no. 3, pp. 1536–1545, May 2015.

[28] K. Rahbar, J. Xu, and R. Zhang, "Real-time energy storage management for renewable integration in microgrid: An off-line optimization approach," *IEEE Trans. Smart Grid*, vol. 6, no. 1, pp. 124–134, Jan. 2015.

[29] Y. Xu and W. Liu, "Novel multi agent based load restoration algorithm for microgrids," *IEEE Trans. Smart Grid*, vol. 2, no. 1, pp. 152–161, Mar. 2011.

[30] F. L. Lewis, D. Vrabie, and V. L. Syrmos, *Optimal Control*, 3rd ed. Hoboken, NJ, USA: Wiley, 2012, pp. 152–155.

[31] C. R. Robinson, P. Mendham, and T. Clarke, "MACSimJX: A tool for enabling agent modelling with Simulink using JADE," *J. Phys. Agents*, vol. 4, no. 3, pp. 1–7, 2010.

[32] W. T. Elsayed and E. F. El-Saadany, "A fully decentralized approach for solving the economic dispatch problem," *IEEE Trans. Power Syst.*, vol. 30, no. 4, pp. 2179–2189, Jul. 2015.

Yinliang Xu (M'13) received the B.S. and M.S. degrees in control science and engineering from the Harbin Institute of Technology, China, in 2007 and 2009, respectively, and the Ph.D. degree in electrical and computer engineering from New Mexico State University, Las Cruces, NM, USA, in 2013.

From 2013 to 2014, he was a Visiting Scholar with the Department of Electrical and Computer Engineering, Carnegie Mellon University, Pittsburgh, PA, USA. Since 2013, he has been with Sun Yat-sen University–Carnegie Mellon University (SYSU–CMU) Joint Institute of Engineering, Sun Yat-sen University, Guangzhou, and the SYSU–CMU Shunde International Joint Research Institute, Shunde, China, where he is currently an Assistant Professor and the Director of the Advanced Control in Smart Grid Laboratory, an Associate Professor with the School of Mobile Information Engineering, Sun Yat-Sen University. He is also an Adjunct Assistant Professor with the Department of Electrical and Computer Engineering, Carnegie Mellon University. His research interests include distributed control and optimization of power systems, renewable energy integration, and microgrid modeling and control.

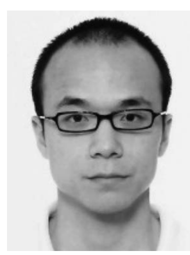

Zaiyue Yang (M'10) received the B.S. and M.S. degrees from the Department of Automation, University of Science and Technology of China, Hefei, China, in 2001 and 2004, respectively, and the Ph.D. degree from the Department of Mechanical Engineering, University of Hong Kong, in 2008.

He worked as a Postdoctoral Fellow and Research Associate with the Department of Applied Mathematics, Hong Kong Polytechnic University, in 2010. He is currently a Professor with Zhejiang University, Hangzhou, China. His current research interests include smart grid, signal processing, and control theory. He is an Associate Editor of the IEEE TRANSACTIONS ON INDUSTRIAL INFORMATICS.

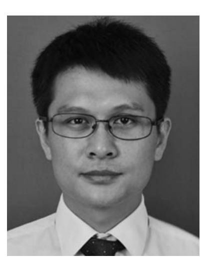

Wei Gu (M'06) received the B.Eng. and Ph.D. degrees in electrical engineering from Southeast University, China, in 2001 and 2006, respectively.

From 2009 to 2010, he was a Visiting Scholar with the Department of Electrical Engineering, Arizona State University, Tempe, AZ, USA. He is currently a Professor with the School of Electrical Engineering, Southeast University. His research interests include distributed generation and microgrids, active distribution networks, and power quality.

Ming Li (M'09) received the B.S. degree in communication engineering from Nanjing University, China, in 2005; the M.S. degree in signal processing from the Institute of Acoustics, Chinese Academy of Sciences, in 2008; and the Ph.D. degree in electrical engineering from USC, in 2013. He joined the Signal Analysis and Interpretation Laboratory, USC, on a Provost fellowship in 2008.

He is currently an Assistant Professor with the Sun Yat-sen University–Carnegie Mellon University Joint Institute of Engineering, and an Associate Professor with the School of Mobile Information Engineering, Sun Yat-Sen University. He is also an Adjunct Assistant Professor with the Department of Electrical and Computer Engineering, Carnegie Mellon University. His research interests are in the areas of speech and language processing, multimodal human behavior signal processing, ultrasound based structure health monitoring, and signal processing in smart grids.

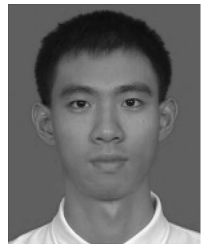

Zicong Deng received the B.S. degree in mathematics and applied mathematics, and the M.S. degree in applied mathematics from Sun Yat-sen University, Guangzhou, China, in 2013 and 2015, respectively. He is currently pursuing the Ph.D. degree with the SYSU–CMU Joint Institute of Engineering, Sun Yat-sen University, Guangzhou, China.

His research interests include control and optimization of microgrids.